GPS-Based Navigation and Orbit Determination for the AMSAT Phase 3D Satellite

Dr. George Davis
Emergent Space Technologies, LLC

Dr. Russell Carpenter, Dr. Michael Moreau, Frank Bauer
NASA Goddard Space Flight Center

Dr. Anne Long, David Kelbel
Computer Sciences Corporation

Thomas Martin
Van Martin Systems, Inc.

Abstract

This paper summarizes the results of processing GPS data from the AMSAT Phase 3D (AP3) satellite for real-time navigation and post-processed orbit determination experiments. AP3 was launched into a geostationary transfer orbit (GTO) on November 16, 2000 from Kourou, French Guiana, and then was maneuvered into its HEO over the next several months. It carries two Trimble TANS Vector GPS receivers for signal reception at apogee and at perigee. Its spin stabilization mode currently makes it favorable to track GPS satellites from the backside of the constellation while at perigee, and to track GPS satellites from below while at perigee. To date, the experiment has demonstrated that it is feasible to use GPS for navigation and orbit determination in HEO, which will be of great benefit to planned and proposed missions that will utilize such orbits for science observations. It has also shown that there are many important operational considerations to take into account. For example, GPS signals can be tracked above the constellation at altitudes as high as 58000 km, but sufficient amplification of those weak signals is needed. Moreover, GPS receivers can track up to 4 GPS satellites at perigee while moving as fast as 9.8 km/sec, but unless the receiver can maintain lock on the signals long enough, point solutions will be difficult to generate. The spin stabilization of AP3, for example, appears to cause signal levels to fluctuate as other antennas on the satellite block the signals. As a result, its TANS Vectors have been unable to lock on to the GPS signals long enough to down load the broadcast ephemeris and then generate position and velocity solutions. AP3 is currently in its eclipse season, and thus most of the spacecraft subsystems have been powered off. In Spring 2002, they will again be powered up and AP3 will be placed into a three-axis stabilization mode. This will significantly enhance the likelihood that point solutions can be generated, and perhaps more important, that the receiver clock can be synchronized to GPS time. This is extremely important for real-time and post-processed orbit determination, where removal of receiver clock bias from the data time tags is needed, for time-tagging of science observations. Current analysis suggests that the inability to generate point solutions has allowed the TANS Vector clock bias to drift freely, being perhaps as large as 5-7 seconds by October, 2001, thus causing up to 50 km of along-track orbit error. The data collected in May, 2002 while in three-axis stabilized mode should provide a significant improvement in the orbit determination results.

Introduction

This report summarizes the efforts to date in processing GPS data from the AMSAT Phase 3D (AP3) satellite. Thus far, the data have been processed primarily to examine GPS satellites tracked, signal levels, Doppler shifts, etc. Selected data sets have also been processed to determine the AP3 orbit from the GPS pseudorange and carrier phase data. The preliminary results suggest that GPS-based orbit determination is feasible for satellites in a highly elliptical orbit (HEO), but there are many important considerations to take into account if such an approach is to operationally support science missions.

AP3 was launched into a geostationary transfer orbit (GTO) on November 16, 2000 from Kourou, French Guiana, and then was maneuvered into its HEO over the next several months. Transponder operation started on May 5, 2001. It carries two Trimble TANS Vector GPS receivers: the A receiver for receiving signals at apogee and the B

receiver for signal reception at perigee. The satellite is currently in a spin-stabilized attitude with the spin axis favorably aligned for getting data from the A receiver throughout the orbit (down toward the earth at apogee, up toward the GPS at perigee). This receiver operates with "random search" acquisition mode. The perigee receiver is not currently turned on.

The AP3 orbit is depicted in Fig.1. Osculating values for the orbit parameters on 10/05/01 are provided in Table 1. The apogee carries AP3 well above the GPS constellation, which has a nominal altitude of about 20,000 km, providing a unique opportunity to track backside signals that skim the Earth's limb. In fact, the TANS Vectors have amplifiers to boost the signal strength for that purpose. The perigee carries AP3 well under the GPS constellation, and into an altitude favorable for tracking 4 or more GPS satellites, as would a receiver in a low earth orbit (LEO). The real-time orbit determination strategy would therefore be to obtain a point positions at perigee to solve for the initial position, velocity, and time bias, and use the values to seed a Kalman filter that could then provide state vector updates even when only one GPS satellite was being tracked.

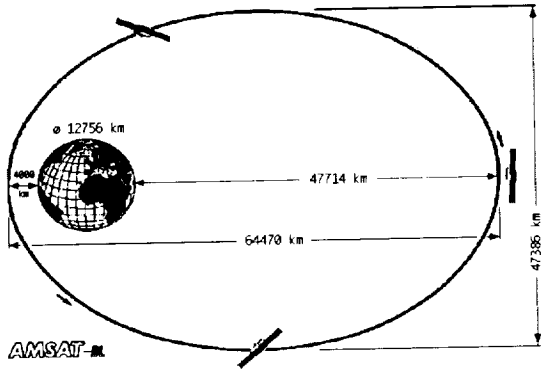

Figure 1. AMSAT Phase 3D Orbit

Table 1. Nominal Orbit Parameters for AP3 on 10/05/1

Orbit Parameter	Value
Epoch of Elements (UTC)	10/05/01 17:05:04.00
Semimajor Axis (m)	36244700.1
Perigee Height (m)	1041850.7
Apogee (Height)	58691275.4
Eccentricity	0.797
Inclination (deg)	6.044
Argument of Perigee (deg)	335.839
Longitude of Ascending Node (deg)	151.818
Mean Anomaly	2.002

Data

The AP3 GPS data received to date at the NASA Goddard Space Flight Center are summarized in Table 1. Blank lines indicate data that have yet to be processed for the purpose of orbit determination, either because the data sets did not appear to have perigee passes with 4 GPS satellites being tracked, or because there were no C-band tracking data for independent verification of orbit accuracy.

Table 1. AMSAT Phase 3D GPS Tracking Data Summary

Date	Time of First Observation	Time of Last Observation	Total GPS Tracked	Max GPS Tracked	No. of 4 GPS Epochs
09/25/01					
09/26/01					

09/27/01	05:45: 9.50	21:28:22.00	12	2	0
10/05/01	03:10:23.50	22:49:56.00	14	4	24
10/06/01					
10/07/01					
10/08/01					
10/09/01					
10/17/01	21:30:45.00	23:59: 1.50	3	1	0
10/18/01					
10/26/01					
10/27/01					
10/28/01					
10/29/01	00:02:26.50	17:25:52.50	14	3	0
10/30/01	00:03:09.00	16:59:22.50	12	3	0
11/01/01					
11/02/01	01:25:47.50	20:59:21.50	8	3	0

To aid in analyzing the AMSAT GPS data, C-band tracking data (range, azimuth, and elevation) were obtained from the Air Force Research Laboratory for processing with the MicroCosm orbit determination software. The data received to date at the NASA Goddard Space Flight Center are summarized in Table 2.

Table 2. AMSAT Phase 3D C-Band Tracking Data Summary

	No. of Observations				
Date	**Range**	**Az**	**El**	**Station(s)**	**GPS**
07/26/01	05	05	05	EGLQ	
07/27/01	00	09	09	MAAQ, MAUQ	
07/29/01	00	03	03	MAUQ	
07/30/01	13	13	12	EGLQ	
07/31/01	00	06	06	MAUQ	
08/04/01	00	06	06	MAUQ	
08/06/01	00	06	06	MAUQ	
08/08/01	00	04	04	MAUQ	
08/10/01	00	03	03	MAUQ	
08/11/01	00	07	07	MAUQ	
08/15/01	00	02	02	MAAQ	
08/20/01	00	06	06	MAUQ	
08/22/01	00	03	03	MAUQ	
08/23/01	00	11	11	MAAQ, MAUQ	
08/24/01	00	12	12	MAAQ, MAUQ	
08/25/01	00	09	09	STAQ, SOCQ, MAAQ	
08/26/01	00	07	07	SOCQ, FYLT, GARQ	
08/27/01	00	03	03	MAAQ	
08/29/01	00	03	03	MAAQ	
09/01/01	00	03	03	SOCQ	
09/02/01	00	06	06	MAAQ	
09/03/01	00	02	02	STAQ	
09/04/01	00	03	03	MAAQ	
09/05/01	00	09	09	MAAQ, STAQ	
09/06/01	00	06	06	MAAQ	
09/08/01	00	06	06	MAAQ	
09/09/01	00	06	06	SOCQ, STAQ	
09/10/01	00	06	06	MAAQ, MAUQ	
09/11/01	00	04	04	MAAQ, SOCQ	
09/12/01	00	06	06	MAUQ	
09/15/01	09	09	09	EGLQ	

09/18/01	00	03	03	MAUQ	
09/19/01	07	07	07	EGLQ	
09/21/01	06	09	09	SOCQ, EGLQ	
09/23/01	00	02	02	STAQ	
09/27/01	14	14	14	EGLQ	•
10/14/01	00	09	09	SOCQ, STAQ, MAUQ, MAAQ	
10/17/01	14	14	14	EGLQ	•
10/21/01	13	13	13	EGLQ	
11/02/01	12	12	11	EGLQ	•
11/03/01	06	06	06	EGLQ	
11/07/01	05	05	05	EGLQ	
11/08/01	00	03	03	STAQ	
11/10/01	13	13	13	EGLQ	
11/11/01	05	08	08	EGLQ	
11/14/01	05	05	05	EGLQ	

Table 2 shows that the C-band data are extremely sparse. Over the 111-day span, C-band tracking data were available on only 46 days, and of those, range data were available only on 14. All the range data come from Eglin Air Force Base (EGLQ) in single station passes per day. The range data are important because their precision is on the order of 1 m, while that of the angle data is considered to be fairly coarse. The range data are needed for computing independent orbits for comparison against the GPS-derived orbits, although their accuracy is limited due having only one pass per day.

Out of the 14 days with C-Band range data, GPS data were available only on 3 days (09/27/01, 10/17/01, and 11/02/01). As can be seen from Table 1, none of these days yielded GPS data in which at least 4 satellites were tracked. In fact, of the GPS data processed so far, the tracking of 4 GPS satellites has been observed only on 10/05/01. Unfortunately, as can be seen from Table 2, this day is in the middle of a large span in which no C-band data were available at all.

Pseudorange Recovery

The TANS Vector reports the following GPS observables: code phase, carrier phase, and Doppler. The code phase is related to the pseudorange, which is used to compute point positions or navigation solutions. The pseudorange is also the fundamental tracking observable used by the GEODE Kalman filter.

The pseudorange represents the number of integer and fractional C/A code repeats measured between signal transmission by the GPS satellite and reception by the GPS receiver. The code phase is the pseudorange modulo the C/A code length, i.e., the receiver truncates all integer number of C/A code repeats in the measurement and reports only the fractional part. The code phase is a compact means of reporting pseudorange because the line-of-sight distance from any particular GPS satellite to a host vehicle is sufficiently far that the first several digits change little, even over long periods of time.

To recover the pseudorange, the line-of-sight range between the receiver and the transmitter must be known, as well as the receiver clock bias. If the receiver is computing navigation solutions, which it would if it were in LEO, then the receiver position and clock bias would be known. The GPS satellite positions are known from the broadcast ephemeris. Differencing the two and taking the magnitude yields the geometric range. The effects of receiver and GPS clock biases must then be taken into account. The former are generally much larger than the latter. Again, if the TANS Vector were computing point positions, which it would if it were in LEO, it would be able to maintain its bias to within ±1 millisecond of GPS time. At its maximum, this translates into about ±300 km of range error, the magnitude of which is equivalent to the length of a C/A code interval.

Now, the C/A code repeats 1023 times every millisecond, yield a chipping rate of 1.023×10^3 chips/sec. The speed of light is assumed to be the WGS-84 value of 2.99792458×10^8 m/sec. Dividing the speed of light by the C/A code chipping rate then yields the C/A-code chip length, or 293 m/chip. This relationship allows the code phase reported by the TANS Vector, which is given in units of $1/16^{th}$ of a C/A chip, to be converted to meters. Multiplying the chip length by 1023 yields approximately 300 km per C/A code repeat interval.

The algorithm for recovering pseudorange from the code phase is a follows:

(1) Get the receiver position, $\vec{x}_r$, and clock bias, Δt_r, from the point solutions (for AP3, no point solutions were available, so an external ephemeris was obtained from the NORAD two-line elements, and the clock bias was assumed to be zero)

(2) Get the GPS satellite position, $\vec{x}_{GPS}$, from the broadcast ephemeris (these can also be obtained from IGS precise orbits, but interpolation would be required)

(3) Compute the geometric range, $r_{geom} = \left\| \vec{x}_{GPS} - \vec{x}_r \right\|$

(4) Compute the computed range, $r_{comp} = r_{geom} + c * \left(\Delta t_r - \Delta t_{GPS} \right)$

(5) Convert the observed code phase from $1/16^{th}$ chips to meters, $\rho_{obs} = \left(\rho_{raw} / 16 \right) * \left(c * t_{CA} / n_{chips} \right)$

(6) Compute the ambiguous number of C/A code repeats, $n_{rep} = \left(r_{comp} - \rho_{obs} \right) / \left(c * t_{CA} \right)$

(7) Form the observed pseudorange, $\rho = n_{rep} * c * t_{CA} + \rho_{obs}$

where

$c = 2.99792458 \times 10^8$ m/sec
Δt_r = receiver clock bias in seconds
Δt_{GPS} = GPS clock bias in seconds
ρ_{raw} = raw code phase in $1/16^{th}$ chips
$t_{CA} = 1 \times 10^{-3}$ sec
$n_{chips} = 1023$

From equations 1 through 4, it is clear that there are 4 sources of error in reconstructing the pseudorange from the code phase: $\vec{x}_r$, $\vec{x}_{GPS}$, Δt_r, and Δt_{GPS}. The combined effect of these errors can not be larger than the length of a C/A code repeat interval, or 300 km, otherwise they would inadvertently introduce a spurious 300 km into the pseudorange.

If the AMSAT receiver were generating point positions, then the receiver position would be known to within the Standard Positioning System (SPS) limits. In general, this would be on the order of 20 m. For AMSAT, however, the receiver has been unable to compute position solutions. Its HEO makes it such that 4 or more GPS satellites are visible only around perigee, and the spin stabilization causes signal levels to fluctuate as other antennas on the satellite block the signals. As a result, point solutions are not available, requiring ephemerides from NORAD TLEs to be used instead.

Generating an ephemeris from a NORAD TLE is based upon the SGP4/SDP4 analytical solution developed by Dr. David Vallado at the Air Force Research Laboratory. The SGP4 algorithm is used for NORAD-tracked objects with periods of less than 225 minutes. For periods greater than this, the deep space SDP4 algorithm is used. These algorithms are needed to properly extract the Earth-fixed position and velocity from the NORAD TLE. It should be noted, however, that the TLEs themselves are based on the same sparse C-band tracking data shown in Table 2, so there can obviously be times when the TLEs are more and less accurate. For example, the ephemeris obtained for 10/05/01 processing is likely of poor quality since there is such a long drop out of data before and after that time.

To assess the accuracy of the TLEs, various ephemerides were computed and compared to one another. First, the AMSAT ephemeris on 10/05/1 was computed from the TLE using Vallado's SDP4 and using the SGP4 algorithm in Satellite Toolkit (STK). This was because the Vallado code outputs the ephemeris in an ECI frame, but the reconstruction of the pseudorange assumes an ECF frame. A simple rotation about the Z-axis using the Greenwich Hour Angle was then applied to the SDP4 ECI ephemeris. The STK ECI ephemeris is transformed internal to the program. The results are summarized in Table 4. It can be seen that the two orbits agree at the km-level, with most of the error being due to an along-track bias. This is likely due to slight misalignments of the two ECF frames. Regardless, orbit error of this magnitude would be negligible in reconstructing the AP3 pseudorange.

Table 4. AP3 Orbit Comparisons: Vallado SDP4/TLE vs. STK SGP4/TLE
10/05/2001

Mean			Std. Dev.			Mean			Std. Dev.		
X	Y	Z	X	Y	Z	R	I	C	R	I	C
0.9	-2.2	-0.4	3.2	3.4	0.2	0.0	-5.5	0.0	0.0	1.8	0.0

- units in km

Next, the ephemeris output by the Vallado SDP4 algorithm was compared to the ephemeris generated by filtering those same positions using MicroCosm. Position data that are used as observations in MicroCosm are known as PCE data, and generally are used to obtain a good reference orbit for processing tracking observables. This enables precise models of gravity, drag, radiation pressure, third body effects, etc. to be included. The results are shown in Table 5. It can be seen that the orbits agree at the km-level, but now there is a bias in the radial direction. This is likely due to differences in the value of GM, which for Vallado is the WGS-72 value and for MicroCosm is the JGM-3 value. Again, orbit error of this magnitude would be negligible in reconstructing the AP3 pseudorange.

Table 5. AP3 Orbit Comparisons: Vallado SDP4/TLE vs. MicroCosm PCE/TLE
10/05/2001

Mean			Std. Dev.			Mean			Std. Dev.		
X	Y	Z	X	Y	Z	R	I	C	R	I	C
3.9	-0.3	0.0	7.6	5.1	1.2	5.4	0.2	-0.2	3.3	7.7	0.7

- units in km

With no C-band tracking data on 10/05/01, similar comparisons were made on 09/27/01, which from Table 2 it is seen that range data from EGLQ are available on that day. The results for the SDP4/TLE orbit versus the MicroCosm PCE/TLE orbit are shown in Table 6. The results are strikingly similar to those obtained on 10/05/01, suggesting that the orbit differences are systematic and due to force model and reference frame differences that persist over time.

Table 6. AMSAT Orbit Comparisons: Vallado SDP4/TLE vs. MicroCosm PCE/TLE
09/27/2001

Mean			Std. Dev.			Mean			Std. Dev.		
X	Y	Z	X	Y	Z	R	I	C	R	I	C
-1.5	1.1	0.0	6.1	5.6	1.2	-3.1	-0.2	0.2	3.5	7.1	0.9

- units in km

The results for the SDP4/TLE orbit versus the MicroCosm C-Band orbit are shown in Table 7. It can be seen that the differences are much larger relative to those in Tables 5 and 6, mostly due to a -31 km bias in the along-track direction. This is interesting because the initial orbit used in processing the C-Band data was that obtained from processing the PCE data.

Table 7. AMSAT Orbit Comparisons: Vallado SGP4/TLE vs. MicroCosm C-Band
09/27/2001

Mean			Std. Dev.			Mean			Std. Dev.		
X	Y	Z	X	Y	Z	R	I	C	R	I	C
-12.1	-16.0	-3.3	22.3	20.8	2.4	-3.8	-31.4	0.5	2.8	18.4	0.8

- units in km

The results for the MicroCosm PCE/TLE orbit versus the MicroCosm C-Band orbit are shown in Table 8. It can be seen that the differences are comparable to those obtained when the Vallado SGP4/TLE orbit is compared to the MicroCosm C-Band. This suggests that differences are due to the MicroCosm C-Band data, which is not to be unexpected given that only one pass of data was available.

Table 8. AMSAT Orbit Comparisons: MicroCosm PCE/TLE vs. MicroCosm C-Band

09/27/2001

Mean			Std. Dev.			Mean			Std. Dev.		
X	Y	Z	X	Y	Z	R	I	C	R	I	C
-3.6	-25.1	-2.4	24.1	25.5	3.2	-6.1	-37.1	0.2	12.2	18.2	1.6

- units in km

To check the consistency of the Vallado SGP4/TLE propagator, three consecutive TLEs were obtained and ephemerides in ECF coordinates were generated over 3 day intervals at 10 second spacing. Comparisons of these orbits were then made at the overlapping points. The results are shown in Tables 9-11. In the first case, shown in Table 9, the TLE epochs were different by about 38 hours, resulting on an overlap of about 34 hours. In the second case, shown in Table 10, the TLE epochs were different by about 19 hours, resulting in an overlap of about 53 hours. In the third case, shown in Table 11, the TLE epochs were different by about 57 hours, resulting in an overlap of about 15 hours. It can be seen that the TLE orbits are consistent at the level of 5 km at the overlapping points.

Table 9. AMSAT Orbit Comparisons: Vallado SGP4/TLE vs. Vallado SGP4/TLE Epoch 10/05/2001 17:05:03.55 vs. Epoch 10/07/2001 07:17:57.71

Mean			Std. Dev.			Mean			Std. Dev.		
X	Y	Z	X	Y	Z	R	I	C	R	I	C
2.0	-0.7	0.8	1.1	2.1	0.5	0.2	2.6	-0.8	1.7	1.0	0.4

- units in km

Table 10. AMSAT Orbit Comparisons: Vallado SGP4/TLE vs. Vallado SGP4/TLE Epoch 10/05/2001 17:05:03.55 vs. Epoch 10/08/2001 02:24:22.47

Mean			Std. Dev.			Mean			Std. Dev.		
X	Y	Z	X	Y	Z	R	I	C	R	I	C
5.4	3.3	0.2	1.7	2.4	0.4	1.3	6.3	0.0	2.4	1.1	0.0

- units in km

Table 11. AMSAT Orbit Comparisons: Vallado SGP4/TLE vs. Vallado SGP4/TLE Epoch 10/07/2001 07:17:57.71 vs. Epoch 10/08/2001 02:24:22.47

Mean			Std. Dev.			Mean			Std. Dev.		
X	Y	Z	X	Y	Z	R	I	C	R	I	C
0.0	1.8	-0.6	3.1	2.1	0.3	0.3	3.8	0.8	1.4	0.6	0.4

- units in km

The above comparisons suggest that without point positions from the AP3T TANS Vector receivers, an external ephemeris based on the NORAD TLE and the SDP4 algorithm is probably no better than 5 km and worse than 50 km. This is well within the 300 km tolerance of the C/A code repeat interval.

Errors in GPS satellite positions obtained from the broadcast ephemeris could also contribute to errors in recovering the pseudorange form the code phase. However, such errors are known to on the order of 20 m for the SPS. As shown in Table 12, comparisons of GPS positions obtained from the broadcast ephemeris those obtained from IGS precise orbits yield differences on the order of 10-30 m. Since the IGS orbits are deemed to be accurate to within 50 cm, these comparisons demonstrate the accuracy of GPS broadcast orbits and eliminate them as sources of error in reconstructing the pseudorange.

Table 12. Comparison of GPS Broadcast Orbits to IGS Precise Orbits 10/05/01

PRN	RSS Position Difference (m)	PRN	RSS Position Difference (m)
01	14.731	17	18.869
02	15.814	18	13.684
03	14.876	20	15.603
04	11.819	21	24.835

05	17.882	22	17.112
06	17.128	23	29.850
07	17.517	24	14.252
08	13.690	25	14.382
09	12.623	26	13.242
10	13.759	27	12.907
11	16.243	28	15.680
13	14.988	29	13.362
14	16.132	30	13.438
15	15.906	31	15.435

As with the GPS broadcast ephemeris, it is assumed that the error due to the GPS clocks is also negligible when reconstructing the pseudorange. Quadratic coefficients are provided as part of a clock model in the broadcast message to correct for such error. An examination of the GPS clock errors on 10/05/01 shows that this term can be as small as 1 km and as large as 150 km. However, it is reasonable to assume that the effect is being taken into account correctly, so that regardless of its size, it contributes little to the error in recovering the pseudorange. In fact, the SPS allocates approximately 2 m of ranging error due to the broadcast GPS clocks.

The final source of error to take into consideration is the AMSAT TANS Vector clock bias. If the receiver were computing point positions, it would also compute the clock bias, which from Eq. 4 is seen to be an essential element in recovering the pseudorange. Since the clock bias is scaled by the speed of light, even small errors in the value of the time bias can lead to substantial range errors. When point positions are computed, the TANS Vector maintains the clock bias to within ±1 milliseconds of GPS time. If the clock were to drift outside of this boundary, then it would not be possible to distinguish clock error from orbit error when trying to recover the ambiguous number of C/A chips. To date, no position solutions have been found in the AMSAT GPS data. As a result, the receiver has been unable to adjust its time bias, making it extremely likely that the clock is drifting freely. If the receiver had been able to "fully acquire" even one GPS satellite signal, to the point of downloading its ephemeris, it would have been able to reset its clock to within 1 second of GPS time. Given that a quartz crystal oscillator typically has a stability on the order of 1 part in 10^7, an assumption of a linear drift suggests that the TANS Vector clock could be of by as many as 8.6 milliseconds per day. After 100 days, it could be off by as many as 0.86 seconds, and after 300 days, 2.6 seconds. This would also cause the data time tags to be in error, thus causing along-track errors when trying to fit orbits to them using a filter like MicroCosm.

Orbit Determination

Of the days with GPS tracking data, only 10/05/01 yielded epochs with 4 GPS satellite tracked. This enabled point positions to be computed outside of the receiver, which apparently could not maintain lock long enough to download the broadcast ephemeris for each satellite and thus compute navigation solutions. Broadcast ephemerides were therefore obtained from the IGS and point positions were computed and compared the ephemeris from the SDP4/TLE. The results are summarized in Table 13. The ΔT column refers to fix time biases added to the data time tag to see if the clock bias could be determined empirically. Thus, ΔT=0 refers to the data obtained directly from the receiver with no bias added.

Table 13. AMSAT Point Positions vs. Vallado SGP4/TLE
10/05/2001

	Mean			Std. Dev.			Mean			Std. Dev.			
ΔT	X	Y	Z	X	Y	Z	R	I	C	R	I	C	Max 3D
-9	71.5	31.2	-4.4	4.7	6.4	1.1	49.3	-59.2	9.3	12.1	1.4	1.3	88.5
-7	76.4	8.1	-0.9	3.5	3.9	0.8	28.6	-70.4	10.1	10.1	0.5	1.0	82.8
-5	81.3	-15.0	2.6	2.3	1.3	0.6	7.7	-81.8	5.7	8.2	1.2	0.7	85.6
-3	86.1	-38.2	6.1	1.1	2.3	0.3	-13.2	-93.2	3.8	6.3	2.3	0.4	96.4
-1	90.0	-61.6	9.6	0.2	3.9	0.0	-34.2	-104.6	2.0	4.4	3.5	0.2	112.9
0	93.2	-73.4	11.4	0.8	5.2	0.2	-44.6	-110.5	1.0	3.4	4.2	0.0	122.7
1	95.6	-85.0	13.2	1.5	6.5	0.3	-55.2	-116.2	0.0	2.4	4.1	0.1	133.2
3	100.2	-108.5	16.7	2.7	9.1	0.6	-76.3	-127.8	-1.8	0.5	6.0	0.4	155.8
5	104.8	-132.1	20.3	4.0	11.7	0.9	-97.4	-139.4	-3.7	1.5	7.2	0.7	179.8

- units in km

From Table 13, it can be seen that the computed point positions agree with the SDP4/TLE ephemeris on the order of 100 km, with most of the difference in the along-track direction. Plots of the ECF and RIC orbit differences for $\Delta T=0$ are shown in Figs. 3 and 4, respectively. They are clearly marked by large biases in the radial and along track directions. By adding a fixed number of integer seconds to the time tags, the orbit difference can be reduced to about 80 km, with a a timing bias of about -7 seconds seeming to yield a minimum.

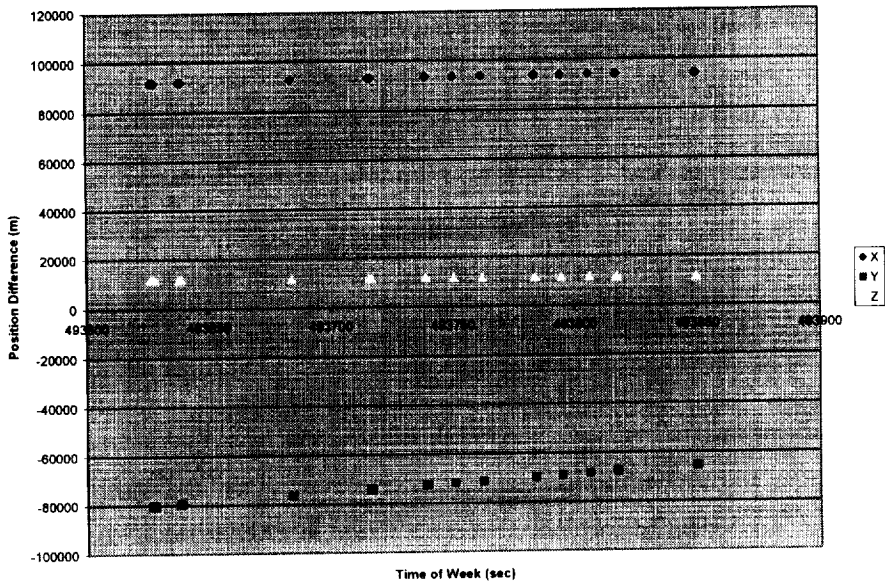

Figure 3. AP3 Point Positions vs. SDP4/TLE in ECF Frame

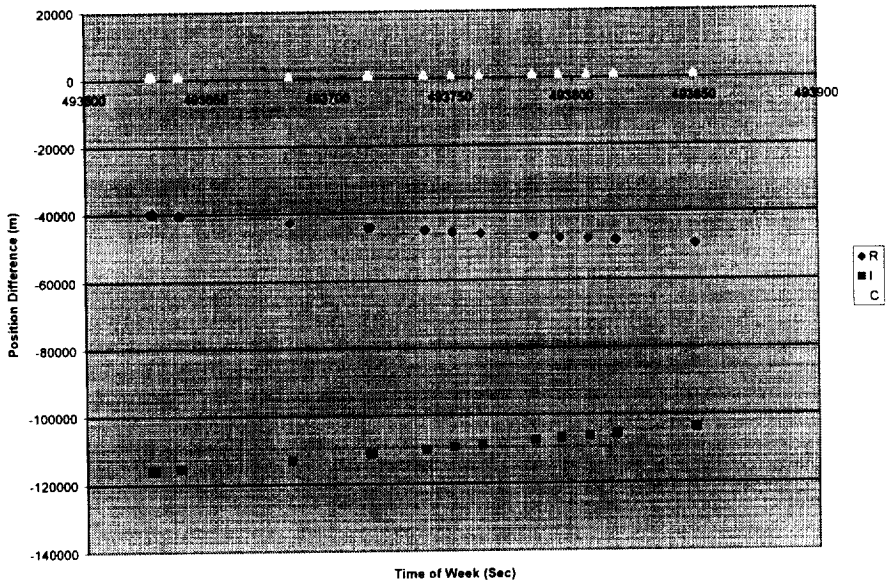

Figure 4. AP3 Point Positions vs. SDP4/TLE in RIC Frame

Given that the AP3 pseudorange is likely corrupted by the unknown clock bias, the next step was to process the carrier phase data, which are reported directly by the receiver and undergo no transformations. To do so, the carrier

phases from 10/05/01 were first processed to generate range-rate data. This is done by differencing consecutive phase measurements and dividing by the time interval. The advantage of processing carrier phase data in this manner is that the phase bias drops out in the differencing, thus greatly reducing the number of parameters to be solved for in the orbit determination process. The disadvantage is that the data are nosier than the undifferenced carrier phase, a result which is negligible considering all the other potential error sources. The processing results for 10/05/01 are shown in Table 14 for the first iteration only.

Table 14. AP3 Range-Rate Processing Results on 10/05/01

Number of Measurements	26025
Mean Residual (m/sec)	-210.12
RMS Residual (m/sec)	212.00
Adjustment in a (m)	419244.3
Adjustment in e (rad)	0.00229
Adjustment in i (deg)	-0.10554
Adjustment in ω (deg)	-5.91927
Adjustment in Ω (deg)	-0.33667
Adjustment in M (deg)	6.05392

From Table 15, it can be seen that the range-rate residuals are dominated by an extremely large bias of about 200 m/sec. For a good orbit fit, this should probably be on the order of cm/sec at most. As a result, the adjustments of the epoch state are unreasonably large, particularly in a, Ω, and M. The same data were then processed but after adjusting the time tags with a 7 sec bias. The results are show in Table 12. Clearly, adding a fixed bias of 7 seconds had little effect. The adjustments in a, Ω, and M improved only marginally.

Table 15. AP3 Range-Rate Processing Results on 10/05/01

Number of Measurements	26025
Mean Residual (m/sec)	-210.30
RMS Residual (m/sec)	212.41
Adjustment in a (m)	418786.3
Adjustment in e (rad)	0.00230
Adjustment in i (deg)	-0.10330
Adjustment in ω (deg)	-5.91116
Adjustment in Ω (deg)	-0.33331
Adjustment in M (deg)	6.04199

Conclusions

The AP3 GPS experiment has demonstrated that GPS signals can be tracked above the constellation at altitudes as high as 58000 km, provided that there is sufficient amplification of those weak signals. Moreover, it has been demonstrated that even a GPS receiver as old, in terms of technology, as the TANS vector can track up to 4 GPS satellites at perigee while moving as fast as 9.8 km/sec. It is likely that the TAN Vector would have tracked even more satellites, and possibly generated navigation solutions, were it not for the spin stabilization employed for attitude control. The spinning appears to cause signal levels to fluctuate as other antennas on the satellite block the signals. As a result, the TANS Vector is unable to lock on to the signal long enough to down load the broadcast ephemeris and thus generate point solutions. This resulted in having to use the NORAD TLE as an external source of ephemeris data when trying to recover the pseudorange. The NORAD TLEs are probably accurate in the 5-50 km range, well within the 300 km tolerance of the C/A code interval. However, the inability to generate point solutions has prevented the TANS Vector from synchronizing its clock to GPS time, thus causing the time bias to drift freely. With time biases of this magnitude, it is not possible to recover pseudoranges from the code phases without guessing or modeling. Trial and error suggest the time bias could be as large 7 seconds by October, 2001, but it is difficult to tell because the reference orbit from the TLE could be in error as much as 50 km. Time tag errors of this magnitude would make it impossible to the fit the carrier phase data as Doppler range-rate using MicroCosm because the reference orbit is not within the linear region. Large delays due to ionospheric distortion at or near perigee also introduce large errors in the carrier phase, which theoretically could be removed using the "code plus carrier" data

type. Attempts at processing this data in MicroCosm were unsuccessful as a result of a crash in its data preprocessor. This approach, however, warrants further investigation.

Recommendations

The AP3 satellite has been powered down as the spacecraft has entered the eclipse season. In the spring of 2002, the spacecraft will be powered up and 3-axis attitude stabilization will be employed, thus greatly increasing the chance that the TANS Vectors will be able to maintain lock long enough to download the GPS ephemerides and compute navigation solutions. Even if this does not happen, the TANS Vectors should be able to synchronize its clock to within 0.5 seconds of GPS time, thus significantly reducing the time bias and thus improving the chance of recovering pseudoranges from the code phases. It is therefore recommended that the time of when the TANS Vectors are powered on be noted by ground control, and that the GPS data obtained as soon after that time be processed.